# Dynamic Gas Temperature Measurement System*

Denny L. Elmore, Woodrow W. Robinson and William B. Watkins
Pratt and Whitney Aircraft Engineering Division

## SUMMARY

The objective of this effort was to develop a gas temperature measurement system with compensated frequency response of 1 KHz and capability to operate in the exhaust of a gas turbine combustor (Figure 1). Results of the initial portions of this effort were reported in the first Hot Section Technology Conference (Reference 1). Further progress in this development effort is summarized in this presentation. Environmental guidelines for this measurement are presented, followed by a preliminary design of the selected measurement method. Transient thermal conduction effects were identified as important; a preliminary finite-element conduction model quantified the errors expected by neglecting conduction. A compensation method was developed to account for effects of conduction and convection. This method was verified in analog electrical simulations, and used to compensate dynamic temperature data from a laboratory combustor and a gas turbine engine. Detailed data compensations are presented. Analysis of error sources in the method were done to derive confidence levels for the compensated data.

## Environmental Guidelines and Sensor Selection

The sensor design and environmental guidelines for this effort are listed in Figure 2. Environmental parameters are representive of a modern gas turbine engine combustor exhaust, and sensor life, accuracy, spatial resolution and vibration capability are nominal goals for experimentation.

The sensor approach chosen for development is shown in Figure 3. The thermocouple employs two wires of different sizes to obtain data necessary for evaluation of the time constant for each wire. If two thermocouples are positioned in close proximity such that both are exposed to the same instantaneous temperature and velocity, the difference in their thermal responses will be governed by their relative diameters. These responses can then be used to obtain time constants for compensating the thermocouples. The unique feature of these wire thermocouples is a beadless laser butt-welded element, which allows the geometry to be modelled as a cylinder in crossflow.

A detailed review of the platinum/rhodium alloys tensile strengths, melting temperatures, emf outputs, thermal conductivities, stresses to rupture, and specific heats was made. Tensile and stress-rupture values are higher for increasing rhodium content, indicating the best thermocouple should have a high rhodium content. The Type B (platinum - 6% rhodium/platinum - 30% rhodium) was selected over the other commercially available thermocouple materials based on its higher emf output, availability, and known fabrication characteristics. Detailed structural analysis revealed that allowable yield stresses contrained design length-to-diameter ratios to less than 6.5 for the support wires and less than 15.5 for the thermocouple elements.

* Work performed under contract NAS3-23154

Probe Thermal Analysis and Compensation Method

A preliminary thermal model of the thermocouple probe wires was generated to evaluate the effects of radiation losses and end conduction losses. Governing equations and the model nodal breakup are shown in Figures 4 and 5 respectively. The physical thermocouple junction, the small wire, and the larger support wires were simulated by a finite difference model. The gas temperatures were assumed to be periodic fluctuations. The worst case gas temperature was assumed to be a mean gas temperature of 1400K ($2520^{o}R$) with fluctuations of $\pm$ 500K ($\pm$ $900^{o}R$). The more realistic case defined in the data acquisition analysis, $\pm$ 65K ($\pm$ $117^{o}R$) was also evaluated. These cases were evaluated at frequencies of 20, 100, and 1000 Hz.

Results of the transient simulations (shown in Figure 6) indicate that radiation heat losses are not significant (less than 10K), but the conduction losses are too large (maximum of 67K) to be ignored and because of structural requirements previously discussed, cannot be reduced by making the wires longer. This discovery required that analysis of the measured temperature data be performed with a second order equation containing both conduction and convection terms, rather than the simplified first order equation containing only convection terms. The second order energy equation is a linear equation in time and space, whereas the first order equation is only time dependent.

A compensation method which accounts for both conduction and convection effects was developed. A second finite difference model using nine nodes (Figure 10) was used for the remainder of the calculations in this effort. The method is outlined in Figure 7 and explained below.

1. The theoretical transfer functions between the 76$\mu$m (3 mil) t/c signal $\theta_1$ and the gas stream signal $a_n$ and the 254$\mu$m (10 mil) t/c signal $\theta_2$ and the gas stream are computed from the finite difference solution of the differential equations for various values of an aerodynamic parameter $\Gamma$, at a number of discrete frequencies falling between the corner frequencies of the two t/c's. These data are then used to compute the theoretical transfer function $H_t(f)$ between the 254$\mu$m (10 mil) t/c and the 76$\mu$m (3 mil) t/c ($\theta_2/\theta_1$) for the corresponding values of $\Gamma$ and frequency. These curves ($\theta_2/\theta_1$) will be used to determine the insitu value of $\Gamma$ from the measured transfer function of $\theta_2/\theta_1$. The process is as follows:

   a. The following parameters are input or already stored in the computer. For the thermocouple wire - L, l, D, d, $\rho_w$, Kw, $Cp_w$, and $\alpha w$. For the gas stream - $\rho_g$, $K_g$, $Cp_g$, $\gamma_g$, $\mu_g$ and $Pr_g$.

   b. The average or mean conditions for the test data for the following variables are entered into the computer:

      T = mean gas temperature
      P = mean gas pressure
      F/A = fuel air ratio
      $f_1$-$f_x$ = frequencies of $f_n$ at which transfer functions will be evaluated
      Mn = Mach No.

   c. The program computes an estimated value of $\Gamma$ based on the test conditions.

d. The program then computes $\zeta_9$, the transfer function between the wire thermocouples and the gas stream, for the 76 $\mu$m (0.003 in.) and the 254 $\mu$m (0.010 in.) thermocouple from 0.5 $\Gamma$ to 1.5 $\Gamma$ in steps of 0.1 $\Gamma$ at frequencies $f_1$ ....., $f_x$ which are user selected to fall in between estimated values of the corner frequencies of the two t/c's. The equations are evaluated until steady state conditions are reached. The computer code determines the sampling interval for each frequency evaluated to ensure mathematical stability of the finite element model and minimize computation time. The normalized ratio of the magnitude of the temperature fluctuation in the wire to the temperature fluctuation of the gas stream ( $\zeta_9 = \theta_n/a_n$) at frequency $f_n$ is determined by locating the maximum peak amplitude after the model has iterated to steady-state conditions. The phase shift ( $\eta_x$) of the temperature fluctuation in the wire is determined by locating the time at which the $\zeta_9$ crossed zero going positive at the beginning of the period in which the model reached steady-state conditions.

e. The data from (d) are then used to compute the theoretical transfer function $\theta_{2n}/\theta_{1n}$ from 0.5 $\Gamma$ to 1.5 $\Gamma$ at frequencies of $f_1$ through $f_x$.

2. Thermocouple test data are digitized into the Fourier system computer, typically 32 to 120 records each of the 76 $\mu$m t/c dynamic signal and the 254 $\mu$m t/c dynamic and dc signals. Each record contains 2048 samples of data. These data are then converted from millivolts to temperature utilizing NBS calibration curve coefficients for type B thermocouples. The 254 $\mu$m dc channel is utilized as the mean for both dynamic data channels in converting the nonlinear t/c mv singals to linearized temperature. These data records are then saved for recall for additional processing or plotting.

3. An ensemble averaged FFT (Fast Fourier Transform) transfer function analysis is then performed on x number of records of the dynamic records to yield the measured value of $\theta_{2n}/\theta_{1n}$ as a function of frequency. The transfer function is computed as the FFT crosspower divided by the FFT autopower of the 76 $\mu$m signal:

$$H_e(f) = \frac{\theta_{1n}\,\theta^*_{2n}}{\theta_{1n}\,\theta^*_{1n}} \rightarrow \frac{\theta_{2n}}{\theta_{1n}}$$

where * = complex conjugate multiplication.

In conjunction with the computation of the measured transfer function, the coherence function is computed and utilized to assess the quality of the measurement. For the 2048 time sample data record lengths utilized 1024 line FFT's are produced. For the typical sampling rate of 4096 Hz, the FFT analyses yield spectral information dc to 2048 Hz in 2 Hz intervals. A standard Hewlett Packard windowing function (P301) is utilized prior to computation of the FFT's. This window is characterized by excellent spectral amplitude accuracy ( $\pm$ 0.1%). Side lobe suppression is $>$ - 70 db at $\pm$ spectral lines and the effective noise bandwidth is 3.4 spectral lines.

4. Each measured value of $\theta_{2n}/\theta_{1n}$ at frequencies $f_n = f_1 - f_x$ are used in

conjunction with the theoretical curves of $\theta_{2n}/\theta_{1n}$ vs $\Gamma$ to determine a measured value of $\Gamma$ (the program interpolates between the 0.1 $\Gamma$ increments computed in (1) above). The arithmetic average obtained for each frequency is taken as the insitu measured value.

5. Using the measured insitu average value of $\Gamma$ obtained in (4), $\zeta_9$, the normalized transfer function (gain $\theta_{1n}/a_n$ and phase $\eta_{1n}$) of the 76 $\mu$m thermocouple with respect to the gas stream temperature is then computed at all frequencies from the 1st spectral line of the FFT spectrum to the Nyquist frequency of the FFT for each discrete frequency contained in the FFT. This is typically from 2 Hz to 2048 Hz in 2 Hz increments. This spectrum is then used to compensate the 76 $\mu$m t/c data as follows.

6. To compute the compensated ensemble averaged power spectral density function, the ensemble averaged auto power spectrum of the 76 $\mu$m (3 mil) t/c obtained in (3) above is divided by the auto power of its compensation spectrum:

$$\frac{\theta_{1n}\ \theta_{1n}^*}{\left(\left[\frac{\theta_{1n}}{a_n}\right]\left[\frac{\theta_{1n}}{a_n}\right]^*\right)} \rightarrow a_n^2$$

where * = complex conjugate multiplication.

Scaling factors for effective noise bandwidth and FFT Fourier symmetry are applied.

7. To compute the compensated instantaneous time waveform, an FFT spectrum is made on a specific data record. This spectrum is then divided by the compensation spectrum. The compensated spectrum is then inverse Fourier transformed to yield the compensated instantaneous time waveform. The software contains information on specific techniques employed to prevent time waveform distortions associated with the inverse Fourier transform. A threshold, in relative db, is applied to the frequency spectrum of the data signal prior to division by the compensation spectrum to prevent errors where the signal to noise ratio is too low.

$$\frac{\theta_{1n}\angle\eta_{1n} + \phi_n}{\left(\frac{\theta_{1n}}{a_n}\right)\angle\eta_{1n}} \rightarrow a_n \angle\phi_n$$

Sensor Test Program

The test program summarized in the following section was based on three test series consisting of (1) System Shakedown and Compensation Verification Lab Tests, (2) Laboratory Burner Tests, and (3) Full Scale F100 Engine Tests (Figure 8). These tests allowed for a step by step checkout and optimization of the various components of the system while allowing for the experimental evaluation and substantiation of sensor guidelines and development effort goals.

Equations were derived for the electrical analog equivalent, passive RC network of the nine node finite difference thermocouple model for use in lab evaluations of the dual t/c approach. Two breadboard nine node RC element network models, one for the 76 $\mu$m (3 mil) and one for the 254 $\mu$m (10 mil) thermocouple were fabricated. The circuits were modeled for the F100 probe geometry operating at the following conditions:

$T_T$ = $1200^oK$ ($1700^oF$)
$P_T$ = 19.7 atm (290 psia)
$M_n$ = 0.233
F/A = 0.02.

Design values of resistance and capacitance for these simulators are shown in Figure 11 . Potentiometers were used for the resistive components and values were set by measurement with a digital ohmmeter ($\pm$ 1%). Values of capacitive components were combinations of standard value capacitors ($\pm$ 10%) and were not measured. Schedule constraints precluded obtaining more precise capacitance values.

The purpose of this test was to determine the compensation spectrum (gain and phase as a function of frequency) of the 76 $\mu$m (3 mil) analog circuit (and the 254 $\mu$m analog circuit) from the measured transfer function taken between the outputs of the analog circuits of the 76 $\mu$m (3 mil) t/c and the 254 $\mu$m (10 mil) circuit (Figure 9 ) utilizing the HOST software and compare it with the known frequency response spectrum (measured single input - single output using conventional FFT techniques). Wideband (1250 Hz BW) random noise was input in these measurements. Because of the lack of precision in the analog circuit components, thermocouple length and diameter values input to the HOST program compensation software were varied until best agreement between the HOST program results and the known compensation spectra were obtained. The conventionally measured spectra were generated by measuring the transfer function between the input and output of the analog circuit using the 256 ensemble averaged FFT transfer function:

$$H(f) = \text{Gain} \angle \text{ phase } (f) = \frac{G_{in}(f) G^*_{out}(f)}{G_{in}(f) G^*_{in}(f)}$$

where * = complex conjugate multiplication

The best match for the 76 $\mu$m (3 mil) t/c was obtained when it was modeled with an element diameter of 74.9 $\mu$m (2.95 mils) and an element length of 711.2 $\mu$m (28.00 mils). The analog circuits were designed to model the t/c as 76.2 $\mu$m (3.00 mils) diameter with a length of 609.6 $\mu$m (24.00 mils). Gain match was within $\pm$ 15% and phase match within + 4.2 to - 0.8 deg. over the frequency range of 4Hz to 1000Hz.

Similarly, for the 254 $\mu$m (0.010 in.) thermocouple case, the following parameters produced the best match of compensation spectra: the diameter was 260.4 $\mu$m (10.25 mils) and the length was 1587.5 $\mu$m (62.5 mils) as opposed to design values of diameter equal to 254 $\mu$m (10 mils) and length equal to 1587.5 $\mu$m (62.5 mils). Gain disagreement for this case was less than $\pm$ 5% out to 100Hz. The compensation program developed under this contract uses the 254 $\mu$m (10 mil) data only out to about 40Hz. The agreement between the two methods is satisfactory despite lack of precision in the capacitance values in the analog model. Experiments performed

with the analog circuits verified that the finite difference models of the thermocouples work as required. Minor discrepancies, due to lack of precision in electrical component values, could easily be corrected, given adequate time and resources.

Subscale combustor probes were fabricated based on the detailed designs shown in Figure 14, which also shows the completed probe. The subscale combustor probe element junctions were inspected to determine the junction's actual dimensions and weld uniformity. Each thermocouple junction was inspected under a Nikon Metaphot microscope at 100X or 200X magnification, Figure 15. Photomicrographs of each junction and a graduated scale were made to measure the junction diameter and uniformity of the wire cross section. Two angular orientations of each wire were photographed 90 degrees apart. A number of different readings of each photograph were obtained to define the mean value and precision of each sample. Measurement uncertainty of the technique is $\pm$ 2 $\mu$m ($9 \times 10^{-5}$ in.) for the 76 $\mu$m elements and 9 $\mu$m ($4 \times 10^{-4}$) for the 254 $\mu$m elements. Effects of these uncertainties on temperature uncertainty were later determined in sensitivity analyses using the completed data reduction method.

The probe was installed and tested in the subscale combustor rig (Figure 16). The probe and a platinum tube used for measuring gas stream total pressure were mounted downstream of the combustor exit plane. The mounting system was retractable so the probe was not in the gas stream except when data were recorded.

Dynamic temperature data and ambient temperature data were recorded on FM tape. The output of each Preston amplifier was double recorded on the FM tape recorder (0.5V rms and 1.0V rms full-scale record level channels). The signal levels were monitored on an oscilloscope and the fixed gain setting(s) of the Preston amplifier(s) were set as necessary to maintain optimum signal levels on the 0.5V rms record channel. Gain settings were correlated with test points to maintain calibration. Data were recorded at ten steady-state combustor test conditions ranging from the minimum conditions obtainable with the combustor facility. Average gas temperatures varied from 1048K ($1887^{\circ}$R) to 1797K ($3235^{\circ}$R). The gas stream Mach number and total pressure was relatively constant at 0.23 and 1.0 atms, respectively.

Figure 17 are uncompensated and compensated dynamic temperature waveforms for the 3 mil thermocouple and test point 10. The uncompensated waveform has maximum fluctuations of approximately $400^{\circ}$F peak to peak with an rms value of $64^{\circ}$F. The compensated waveform has peak to peak fluctuations of approximately $1200^{\circ}$F and an rms value of $281^{\circ}$F. Figure 18 are uncompensated and compensated power spectral density plots for 120 record averages. Signal to noise ratios for compensated signal to compensated ambient noise are $>$18db up to 500Hz, $>$13db up to 1000Hz and $>$10db out to 2000Hz. A noticeable break in the compensated PSD can be seen at 1200Hz; this results from use of an anti-aliasing low-pass filter, and for this reason, signal to noise ratio from 1200 to 2000Hz is actually greater than 10db. Note that a combustor resonance is indicated by the peak at 145Hz.

The full scale test were conducted as planned in an F100 jet engine which was undergoing testing at P&WA's Government Products Division (GPD) test facility. Test conditions for the data which follows were: P = 158 psia, T = $1790^{\circ}$F, M = 0.355. Figure 19 shows the uncompensated and compensated dynamic temperature waveforms. The uncompensated waveform has peak to peak characteristics of about $400^{\circ}$F and rms value of $73^{\circ}$F. The compensated waveform has peak to peak charac-

teristics of greater than 2000°F, and rms value of 393°F. Figure 20 are power spectral density plots of compensated and uncompensated 120 record average data. Signal to noise ratio is >26db to 500Hz,>20db to 1000Hz and >14db to 2000Hz. The signal is basically wide band random, with no evidence of resonance.

Measurement Uncertainty

The overall compensation uncertainty was obtained by room-sum-squaring errors associated with finite-windowing effects in the Fast Fourier Transform, thermocouple element diameter measurement, temperature waveform ratios, and data acquisition/reproduce noise. These errors are shown in Figure 21 for two input waveforms. The 27°F peak to peak/$\sqrt{Hz}$ wideband random waveform and corresponding errors are representative of the signals observed experimentally.

LIST OF SYMBOLS

$\alpha = \dfrac{K_w}{\rho_w C_{pw}}$ = thermal diffusivity of the wire

$L$ = length of thermocouple support wire

$\ell$ = one half of length of smaller thermocouple wire

$D$ = diameter of thermocouple support wire

$d$ = diameter of smaller thermocouple wire

$\rho_w$ = density of thermocouple wire

$K_w$ = thermal conductivity of thermocouple wire

$C_{pw}$ = specific heat of ther thermocouple wire

$\rho_g$ = density of the gas stream

$C_{pg}$ = specific heat of the gas stream

$P_{rg}$ = Prandtl number of gas stream

$U_g$ = velocity of the gas stream

$\mu_g$ = viscosity of the gas stream

$\gamma_g$ = ratio of specific heats of gas stream

$\theta_{1n}$ = amplitude of the 75 $\mu$m (0.003 in.) thermocouple at frequency $f_n$

$\theta_{2n}$ = amplitude of the 254 $\mu$m (0.010 in.) thermocouple at frequency $f_n$

$a_n$ = amplitude of the gas temperature at frequency $f_n$

$\phi_n$ = phase shift of the gas temperature with respect to arbitrary time $t_o$ at frequency $f_n$

$\eta_{1n}$ = phase shift of 76 $\mu$m (0.003 in.) thermocouple with respect to gas temperature at frequency $f_n$

$\eta_{2n}$ = phase shift of 254 $\mu$m(0.010 in.) thermocouple with respect to gas temperature at frequency $f_n$

$\lambda_{1n}$ = phase shift of 76 $\mu$m (0.003 in.) thermocouple at frequency $f_n$ with respect to arbitrary time $t_o$

$\lambda_{2n}$ = phase shift of 254 $\mu$m (0.010 in.) thermocouple at frequency $f_n$ with respect to arbitrary time $t_o$

$$\Gamma = \frac{0.48 k_g P_{rg}^{1/3} U_g^{1/2}}{\left(\frac{\mu_g}{\rho_g}\right)^{1/2} \rho_w C_{pw}} = \text{Aerodynamic parameter}$$

$\zeta$ = Theoretical transfer function (gain and phase) of the wire thermocouple x with respect to the gas temperature at frequency $f_n$

$H_f(f)$ = Theoretical transfer function between large and small thermocouples

$H_e(f)$ = Experimental transfer function between large and small thermocouple signals

$K_g$ = thermal conductivity of the gas stream

## REFERENCES

1. Elmore, D.; "Dynamic Gas Temperature Measurement System", Turbine Engine Hot Section Technology, NASA TM 83022, 1982.

# DYNAMIC GAS TEMPERATURE MEASUREMENT SYSTEM

Objective - Develop a temperature measurement system with:

- Compensated frequency response of 1 KHz
- Operation at jet engine combustor exit

Talk Outline -
- Environmental guidelines and sensor selection
- Transient conduction effects and compensation method
- Test program
  - Compensation checkout
  - Lab burner
  - Engine
- Error analysis
- Summary

FIGURE 1

AV238751

# SENSOR DESIGN AND ENVIRONMENT GUIDELINES

Geometry: Annular combustor, 2 cm $<$ H $<$ 8 cm

Temperature: T $\sim$ 1400°K (2060°F); T′ $\sim$ 500°K (900°F) -

Frequency response: 1 kHz

Pressure: 10 $<$ P $<$ 20 ATM

Flow: v $\sim$ 150 m/s; v′ $\sim$ 50 m/s -

Gas composition: Fuel (nominal jet A) and air

Sensor life: 5 hr minimum

Accuracy: Temperature uncertainty $\leq$ 5% for f $\leq$ 200 Hz

Temperature uncertainty 10% for 200 Hz $<$ f $<$ 1 kHz

Spatial resolution: D $\leq$ 0.5 cm

Vibration: 10g

FIGURE 2

AV252681

# PRELIMINARY DESIGN CONCEPT: DUAL PASSIVE THERMOCOUPLE

- Ratio of T/C responses determines $h_g$

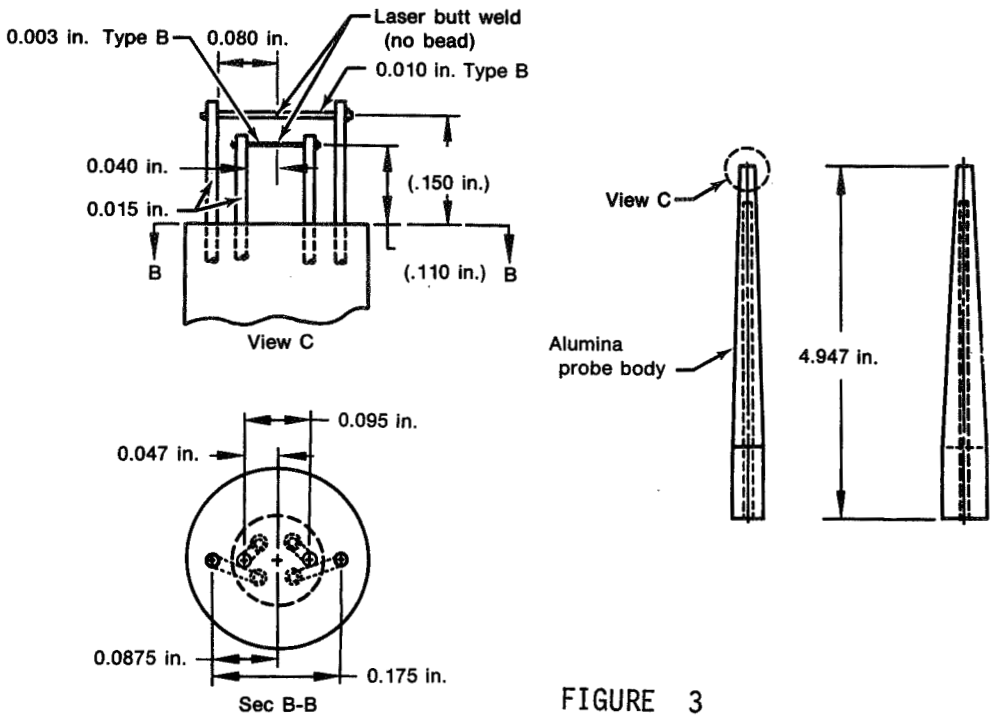


FIGURE 3

AV238759

# FIRST-ORDER AND SECOND-ORDER MODELS COMPARED

## First-order model

Rate of energy change = $Q_{convection} + Q_{radiation}$

$$\frac{dT}{dt} = \frac{4h}{\rho_w c_{pw} D}(Tg - T) + \frac{4\sigma\epsilon}{\rho_w C_{pw} D}(T_e^4 - T^4)$$

## Second-order model

Rate of energy = $Q_{convection} + Q_{conduction} + Q_{radiation}$

$$\frac{dT}{dt} = \frac{4h}{\rho_w c_{pw} D}(Tg - T) + \alpha \frac{\delta^2 T}{\delta x^2} + \frac{4\sigma\epsilon}{\rho_w c_{pw} D}(T_e^4 - T^4)$$

FIGURE 4

AV238777

# PHYSICAL MODEL REPRESENTED BY FINITE DIFFERENCE ANALYTICAL MODEL

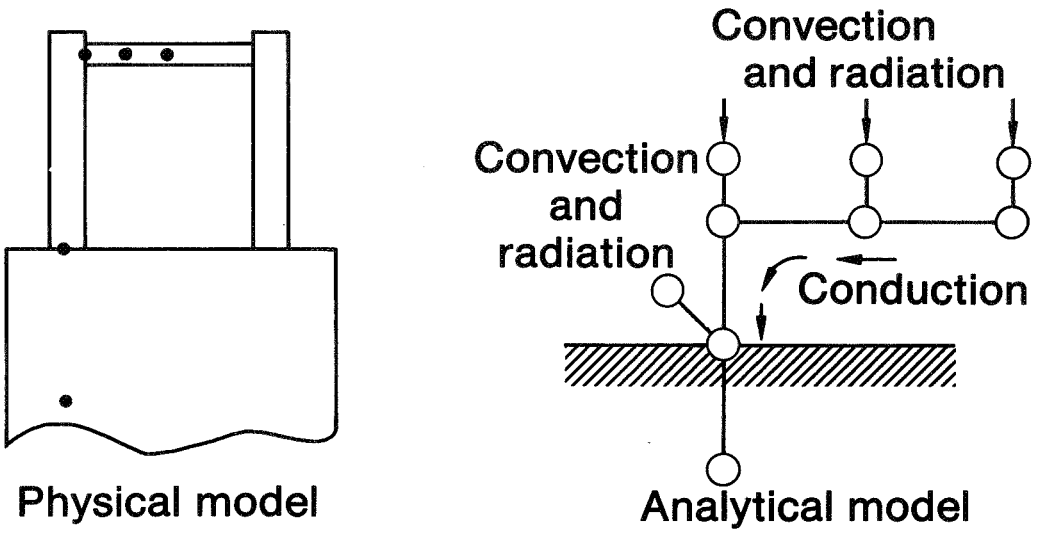


FIGURE 5

AV238776

# MAXIMUM DEVIATION IN PREDICTED JUNCTION TEMPERATURE FROM A 1ST ORDER SYSTEM

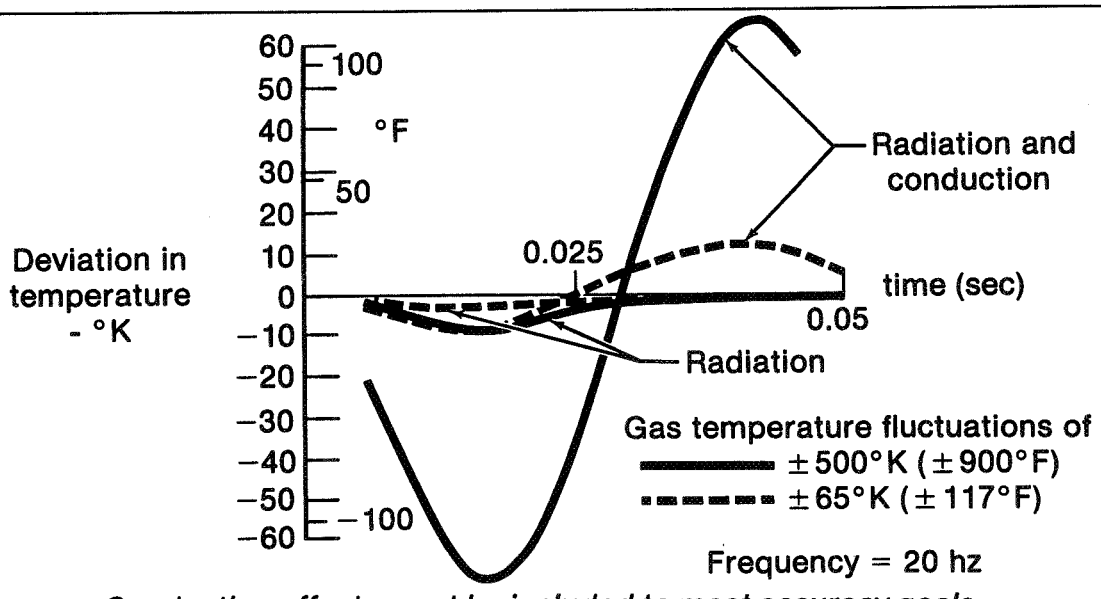


*Conduction effects must be included to meet accuracy goals*

FIGURE 6

AV238785

# COMPENSATION METHOD

- Compute theoretical response (76$\mu$m and 254$\mu$m T/C's) vs heat transfer coefficient (finite element conduction effects included) over frequency range
- Measure (data) response of 76$\mu$m and 254$\mu$m T/C's over frequency range (using FFT techniques)
- Determine actual heat transfer coefficient from computed and measured response
- Generate theoretical response of 76$\mu$m T/C for actual heat transfer coefficient for frequency range
- Compensate 76$\mu$m T/C data in frequency domain
- Inverse Fourier transform to time domain

AV250399

FIGURE 7

# DYNAMIC GAS TEMPERATURE MEASUREMENT SYSTEM

*Test program*

- Compensation method checkout
- Lab burner
- Engine

FIGURE 8

AV260427

# SIMULATION OF DUAL WIRE T/C'S

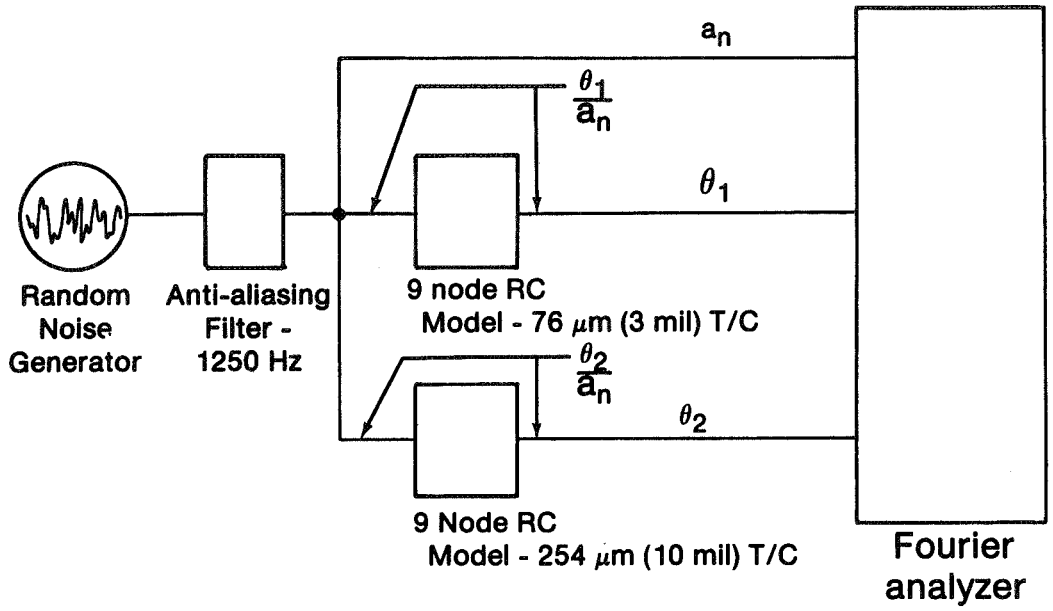


- RC networks modeled as F100 probe
  1200°K (1700°F)
  19.7 ATMS (290 psia)
  Mn = 0.2231
  F/A= 0.02

FIGURE 9

AV257667

# FINITE DIFFERENCE THERMAL MODEL

*Used in computer compensation program*

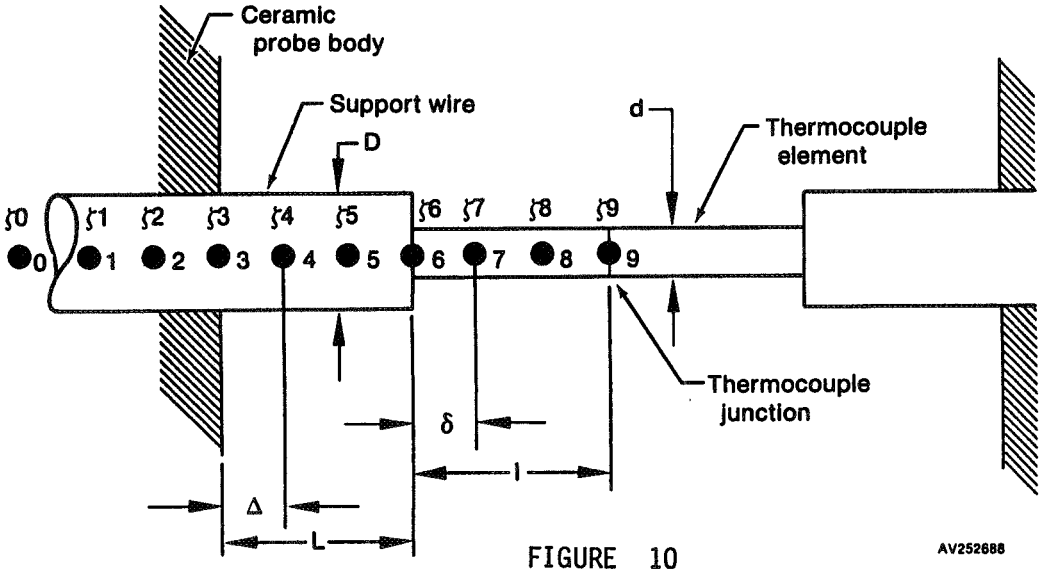


FIGURE 10

AV252688

# RC ANALOG NETWORK SIMULATION

*Full scale test conditions*

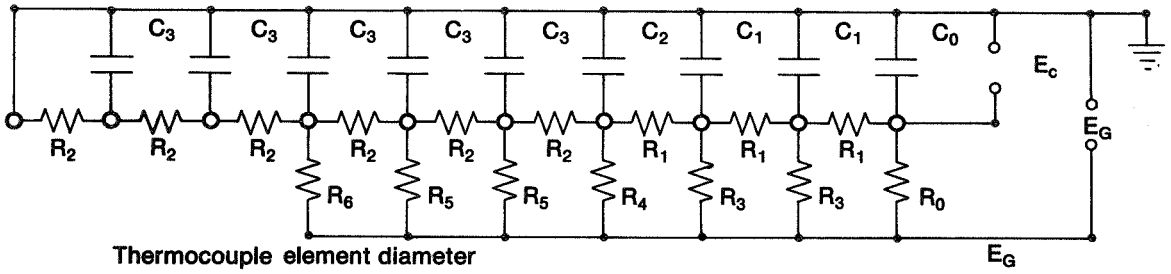


Thermocouple element diameter

| Where: | 76μm | 254μm |
|---|---|---|
| $R_0$ | 7592 Ω | 46.2 KΩ |
| $R_1$ | 1739 Ω | 11.8 KΩ |
| $R_2$ | 217.4 Ω | 5.66 KΩ |
| $R_3$ | 3796 Ω | 23.11 KΩ |
| $R_4$ | 1049 Ω | 12.447 KΩ |
| $R_5$ | 543.5 Ω | 8.515 KΩ |
| $R_6$ | 1087 Ω | 17.031 KΩ |
| $C_0$ | 0.5 μfd | 0.5 μfd |
| $C_1$ | 1.0 μfd | 1.0 μfd |
| $C_2$ | 2.45 μfd | 4.34 μfd |
| $C_3$ | 78 μfd | 7.67 μfd |

Note: Values listed correspond to F100 probe operating at:
$T_T$ = 1200°K (1700°F)
$P_T$ = 19.7 atm (290 psia)
$M_N$ = 0.2331
F/A = 0.02

AV257666 830902 2493B

FIGURE 11

# SIMULATION OF DUAL WIRE TC'S

*76 μm (3 mil) compensation spectrum - measured single input/single output*

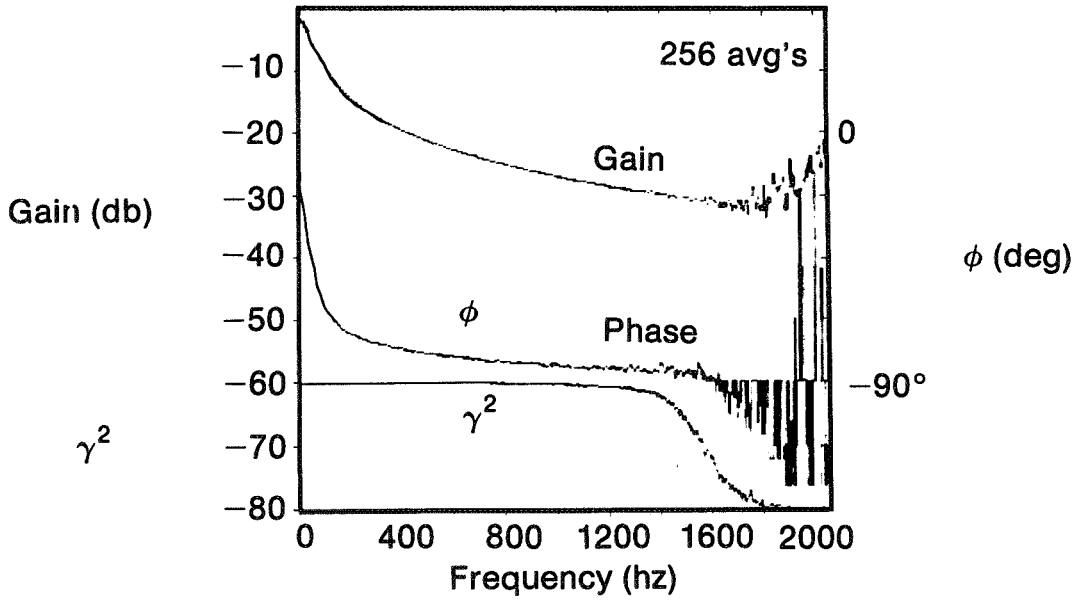


AV260429

FIGURE 12

# SIMULATION OF DUAL WIRE TC'S

*76 μm (3 mil) compensation spectrum - measured dual wire*

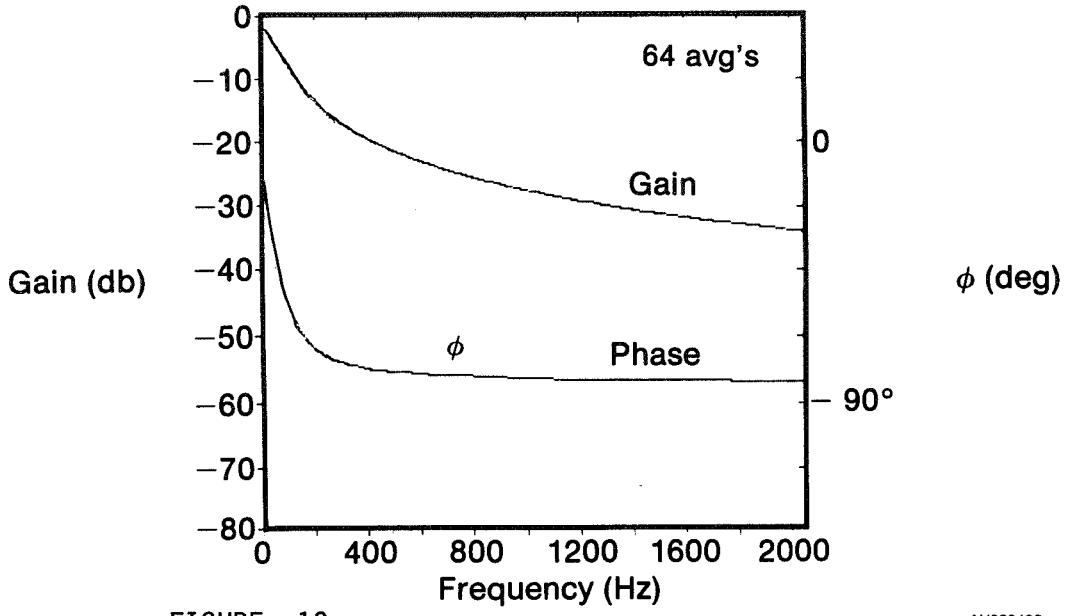


FIGURE 13

AV260428

# SENSOR GEOMETRY

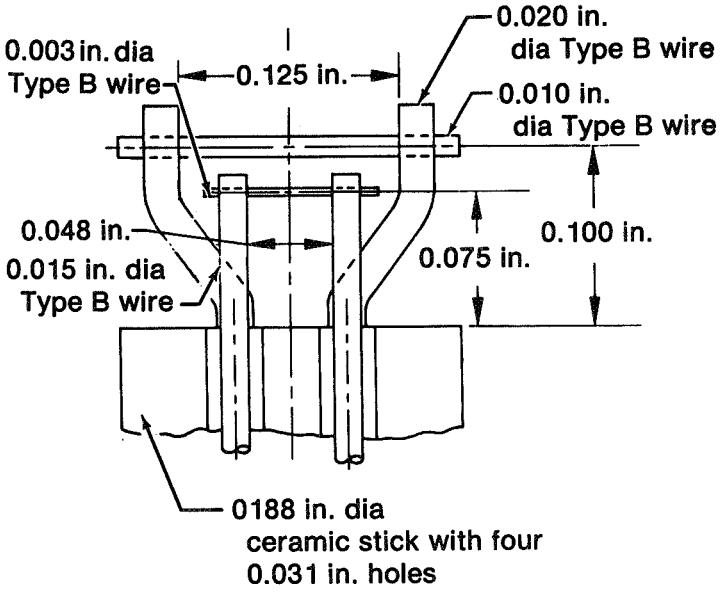


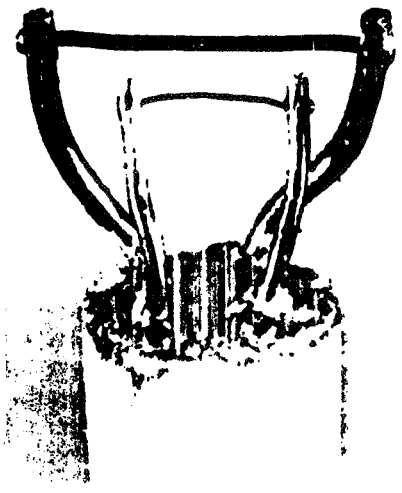

AV260430

FIGURE 14

# MICROSCOPIC INSPECTION OF JUNCTIONS

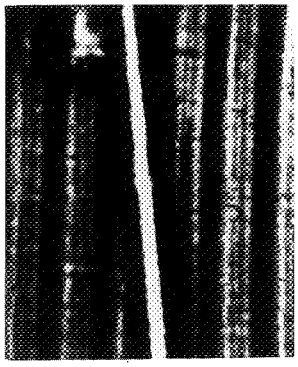

Photomicrograph of 0.003 in. element (200×)

Measured diameter = 0.0029

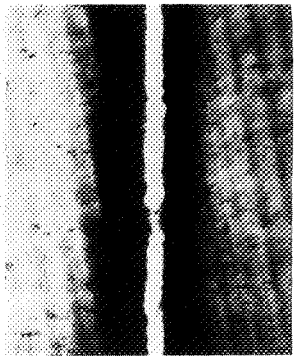

Photomicrograph of 0.010 in. element (100 ×)

Measured diameter = 0.0099

FIGURE 15

AV252691

# SUBSCALE COMBUSTOR RIG TEST DATA

- Test pt. No. 10

  Press = 1.04 atms (15.215 psia)

  Probe $M_n$ = 0.227

  Mean temp = 1837°K (2775°F)

  F/A = 0.025 (est'd)

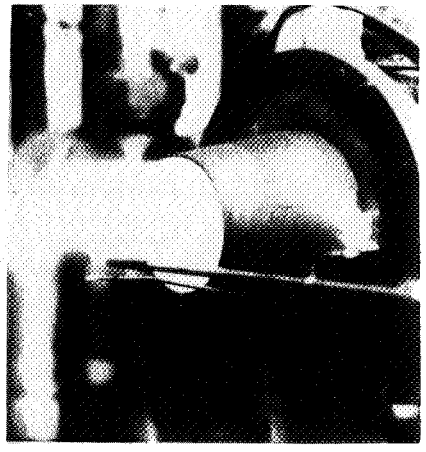

- Ambient - probe retracted/rig running

FIGURE 16

AV260431

# SUBSCALE COMBUSTOR RIG TEST DATA

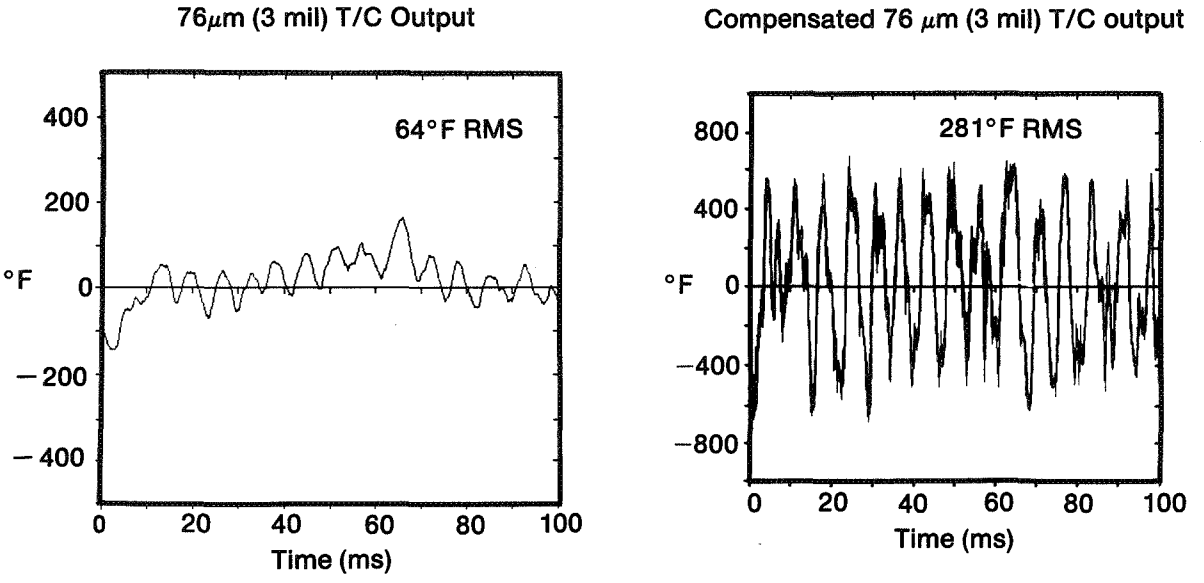


FIGURE 17

AV260432

# SUBSCALE COMBUSTOR RIG TEST DATA

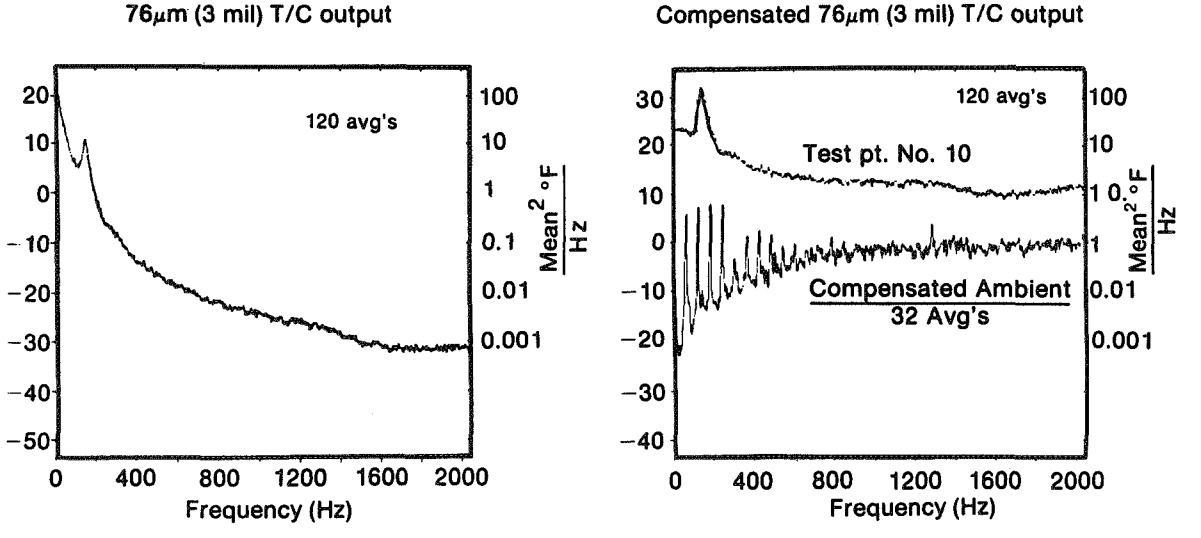


AV260433

FIGURE 18

# F100 TEST DATA

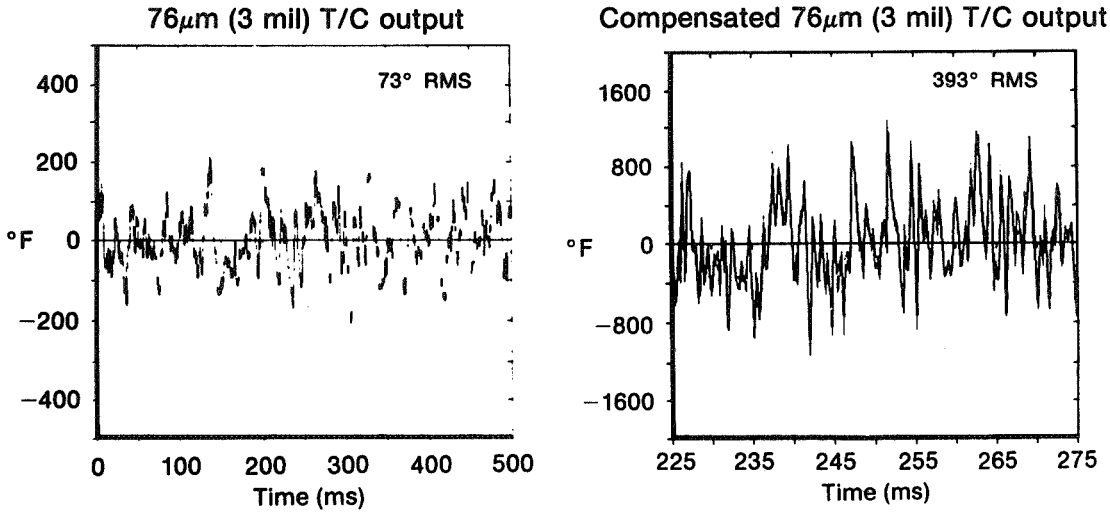


FIGURE 19

AV260434

# F100 TEST DATA

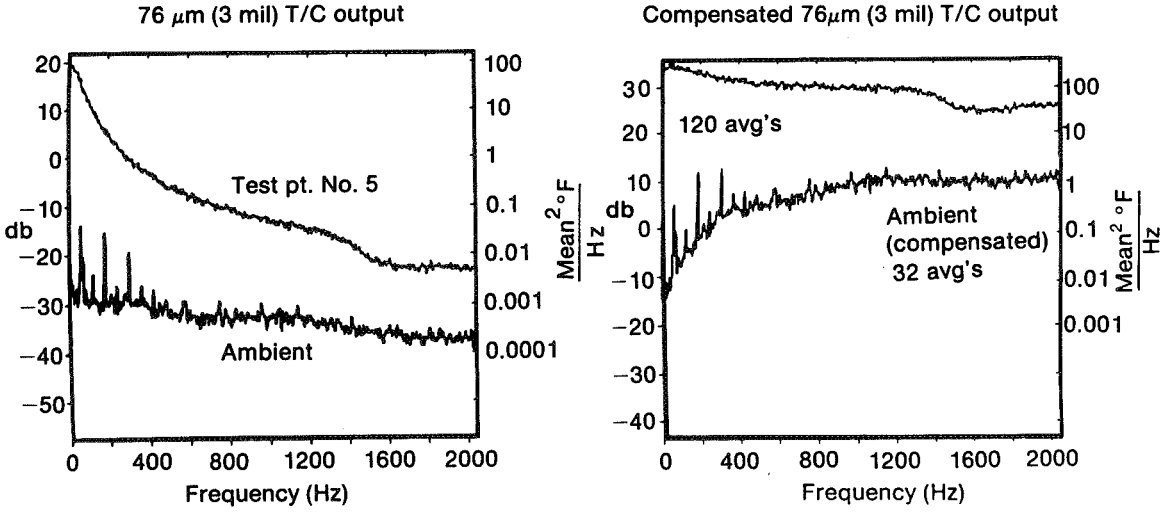


FIGURE 20

AV260435

# DYNAMIC GAS TEMPERATURE MEASUREMENT SYSTEM

**Overall accuracy - instantaneous time waveform**

| | Error due to data system SNR | Compensation technique Error | Error (dia's) | Error ($\theta_2/\theta_1$) | Total error (RSS) |
|---|---|---|---|---|---|
| 1000°K (1800°F) p-p at 200 Hz | <0.1% | 1.6% | 4.9 | 3.3 | 6.1% |
| 1000°K (1800°F) p-p at 1000 Hz | <0.1% | 2.5% | 5.2% | 3.5% | 6.7% |
| ≃ 15°K (27°F) p-p/$\sqrt{}$Hz 4 Hz-200 Hz | 0.7% | 4.4% | 4.9 | 3.3 | 7.4% |
| ≃ 15°K (27°F) p-p/$\sqrt{}$Hz 200 Hz-1000 Hz | 3.8% | 10.6% | 5.2 | 3.5 | 12.9% |

**Overall accuracy - averaged frequency spectrum**

| | Error due to data system SNR | Compensation Error | Error (dia's) | Error ($\theta_2/\theta_1$ | Total error (RSS) |
|---|---|---|---|---|---|
| 1000°K (1800°F) p-p at 200 Hz | <0.1% | 1.1% | 4.9 | 3.3 | 6.0% |
| 1000°K (1800°F) p-p at 1000 Hz | <0.1% | 2.0% | 5.2 | 3.5 | 6.6% |
| ≃ 15°K (27°F) p-p/$\sqrt{}$Hz 4 Hz-200 Hz | 0.7% | 1.2% | 4.9 | 3.3 | 6.1% |
| ≃ 15°K (27°F) p-p/$\sqrt{}$Hz 200 Hz-1000 Hz | 3.8% | 1.9% | 5.2 | 3.5 | 7.6% |

AV260438

FIGURE 21